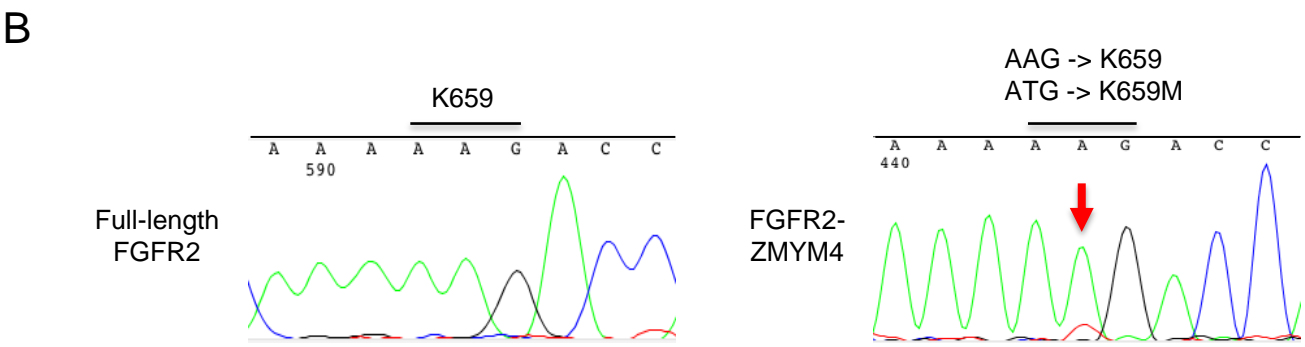
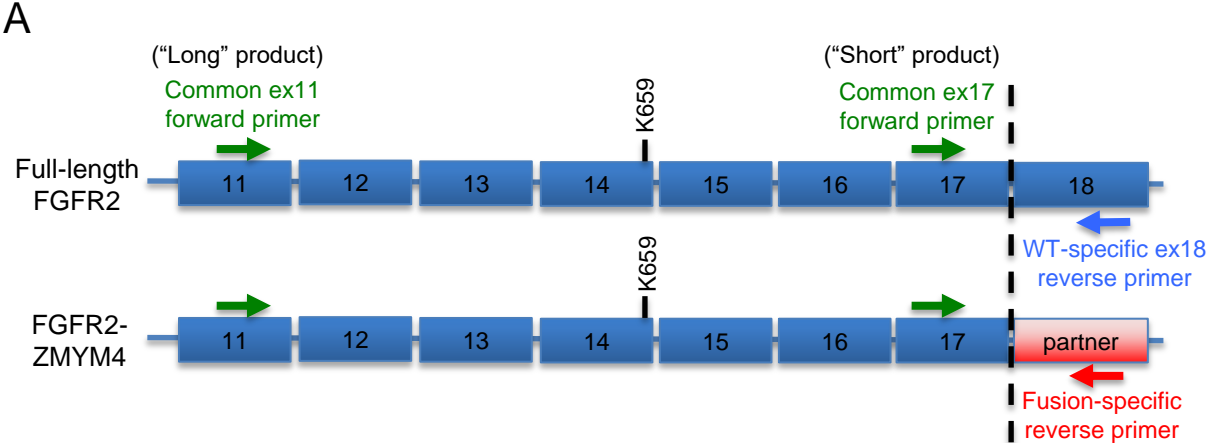


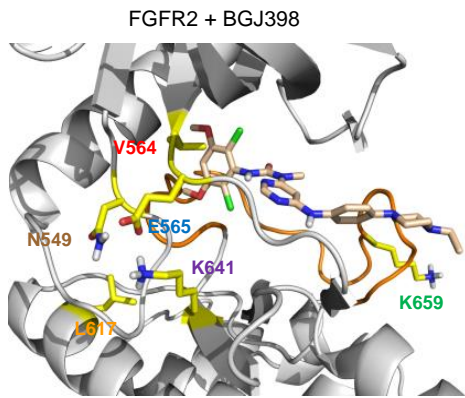
# Supplementary Figure S1



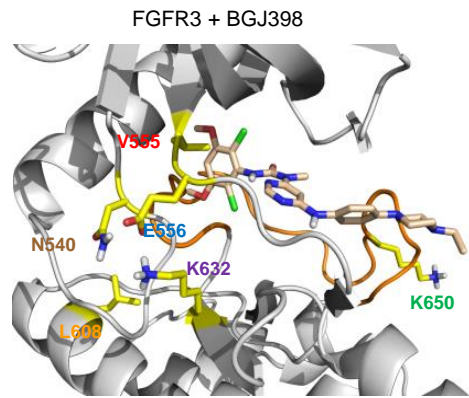
**Supplementary Figure S1. Confirmation of secondary point mutation in FGFR2-ZMYM4 allele. A.** Primers were designed to specifically amplify either full-length FGFR2 or FGFR2-ZMYM4 mRNA from post-progression biopsy tissue of Patient #1. **B.** Sequencing traces from Sanger sequencing demonstrates a K659M mutation in the FGFR2-ZMYM4 allele and not the full-length FGFR2 allele.

# Supplementary Figure S2

A



B



C

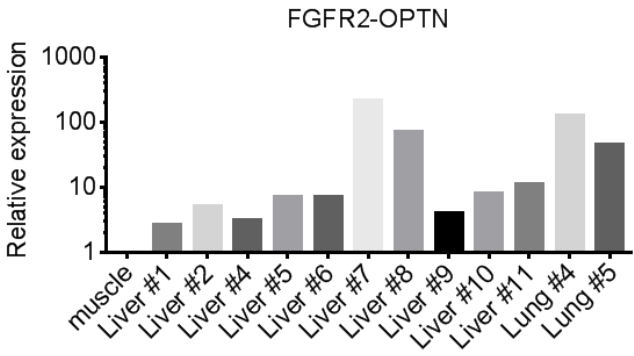
<b>FGFR2</b>	DKLTLGKPLGEGCFGQVVM AEAVGIDKDKPKEAVTVAVKMLKDDATEKDL
<b>FGFR3</b>	ARLTLGKPLGEGCFGQVVM AEAI GIDKDRAAKPVTVAVKMLKDDATDKDL
<b>FGFR2</b>	SDLVSEM EMMKMI GKHKNI I <sup>549</sup> NLLGACTQDGPLYVIVE <sup>564 565</sup> YASKGNLREYLRA
<b>FGFR3</b>	SDLVSEM EMMKMI GKHKNI I NLLGACTQGGPLYVLVEYAAKGNLREFLRA
<b>FGFR2</b>	RRPPGMEYSYDINRVPEEQMTFKDLVSC <sup>617</sup> TYQLARGMEYLASQKCIHRDLA
<b>FGFR3</b>	RRPPGLDYSFDTCKPPEEQMTFKDLVSCAYQVARGMEYLASQKCIHRDLA
<b>FGFR2</b>	ARNVLVTENNVM <sup>641</sup> KIADFG <sup>659</sup> LARDINNIDYYKKT <sup>659</sup> TNGRLPVKWM APEALFDR
<b>FGFR3</b>	ARNVLVTEDNVMKIADFGVLDVHNL DYYKKT <sup>659</sup> TNGRLPVKWM APEALFDR
<b>FGFR2</b>	VYTHQSDVWSFGVLMWEI FTLGGSPYPGIPVEELFKLLKEGHRMDKPANC
<b>FGFR3</b>	VYTHQSDVWSFGVLLWEI FTLGGSPYPGIPVEELFKLLKEGHRMDKPANC
<b>FGFR2</b>	TNELYMMRDCWHAVPSQRPTFKQLVEDLDRILT <sup>659</sup> LTNEE
<b>FGFR3</b>	THDLYMIMRECWHAAAPSQRPTFKQLVEDLDRVLT <sup>659</sup> VTSTDE

## Supplemental Figure S2: Homology between FGFR2 and FGFR3 proteins

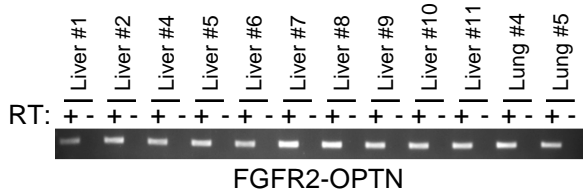
**A and B.** *In silico* model of wild-type FGFR2 (**A**) and FGFR3 (**B**) bound to BGJ398 with relevant amino acids highlighted and color-coded. **C.** Sequence alignment of FGFR2 and FGFR3 indicating sites of specific changes in amino acids due to FGFR kinase mutations.

# Supplementary Figure S3

A



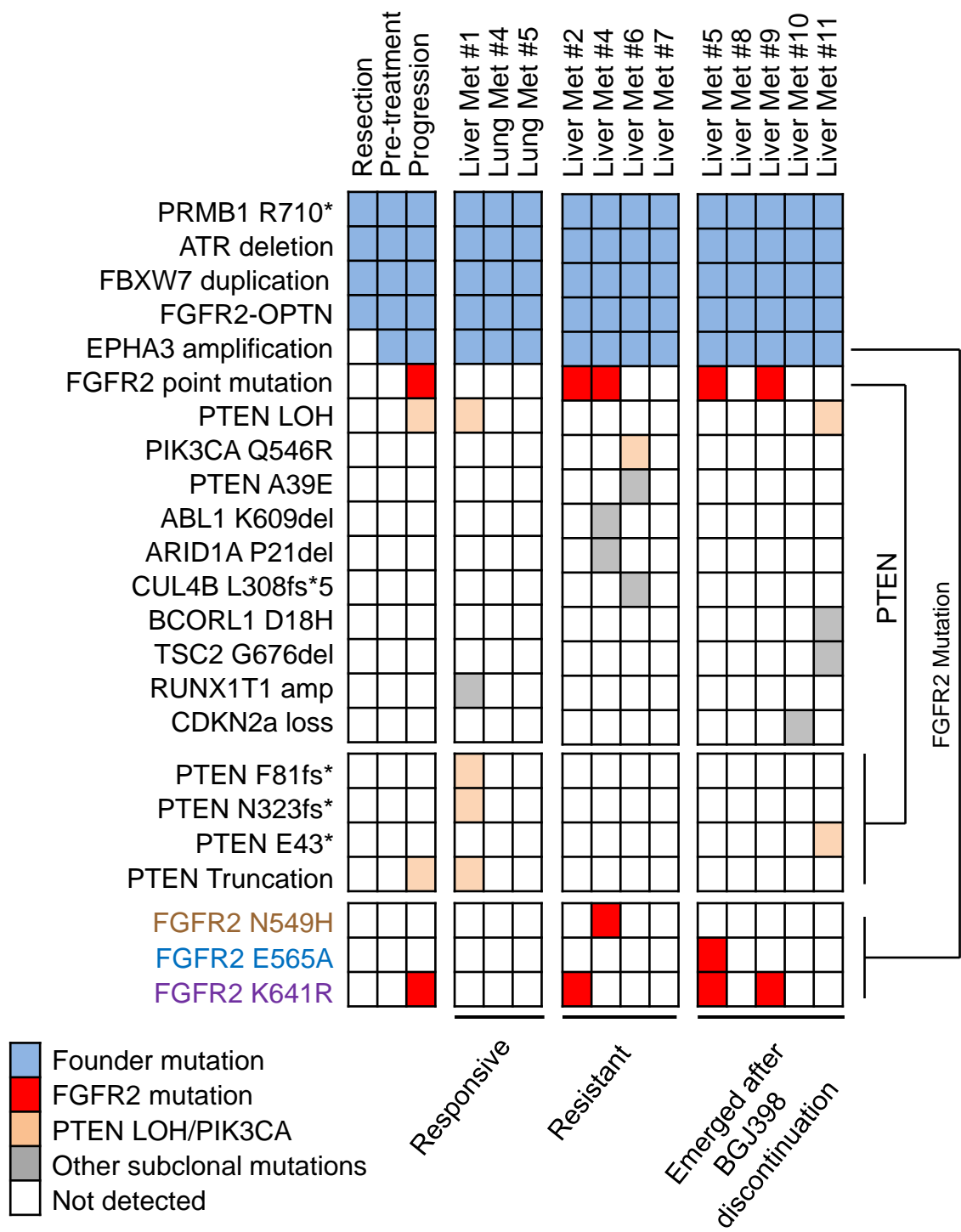
B



**Supplementary Figure S3. FGFR2-OPTN fusion detected in all autopsy lesions.**

**A.** Relative expression of the *FGFR2-OPTN* fusion in the indicated autopsy lesions as measured by real-time quantitative PCR (RT-qPCR). **B.** PCR product isolated from **A**, in the presence or absence of reverse transcriptase (RT), was resolved on an agarose gel.

# Supplementary Figure S4



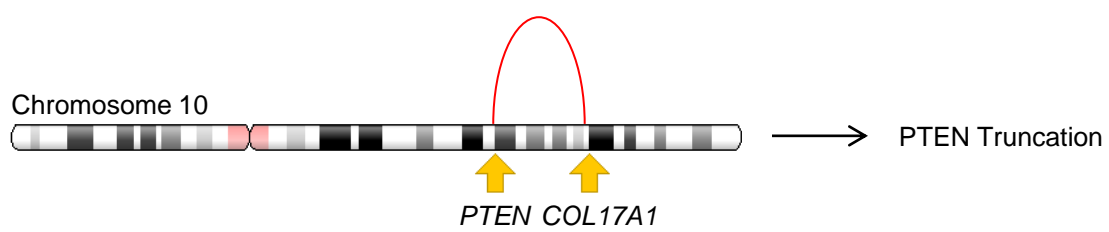
**Supplementary Figure S4. FoundationOne analysis of autopsy lesions**

Heatmap indicating all genetic events identified in the indicated Patient #2 lesions. Gray boxes indicate mutations of undetermined significance.

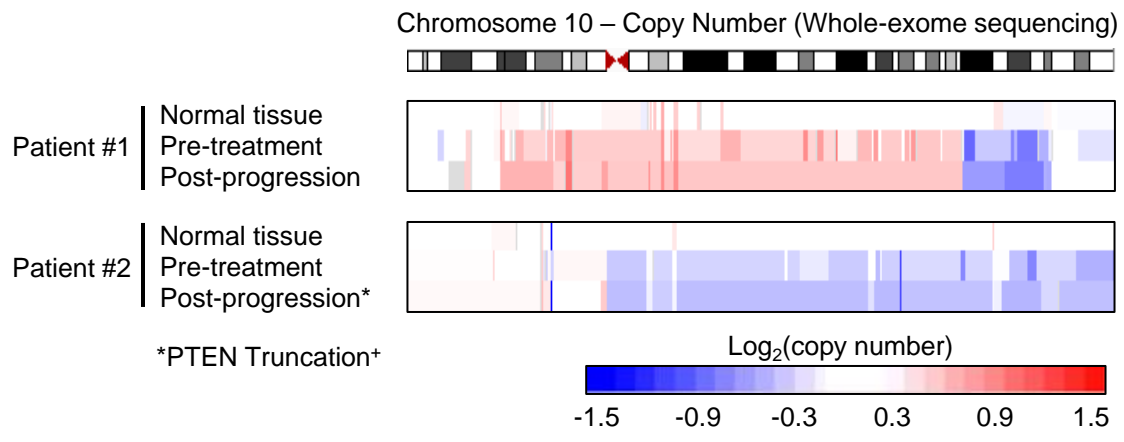
# Supplementary Figure S5

A

Patient #2, Post-Progression Biopsy: FoundationOne analysis



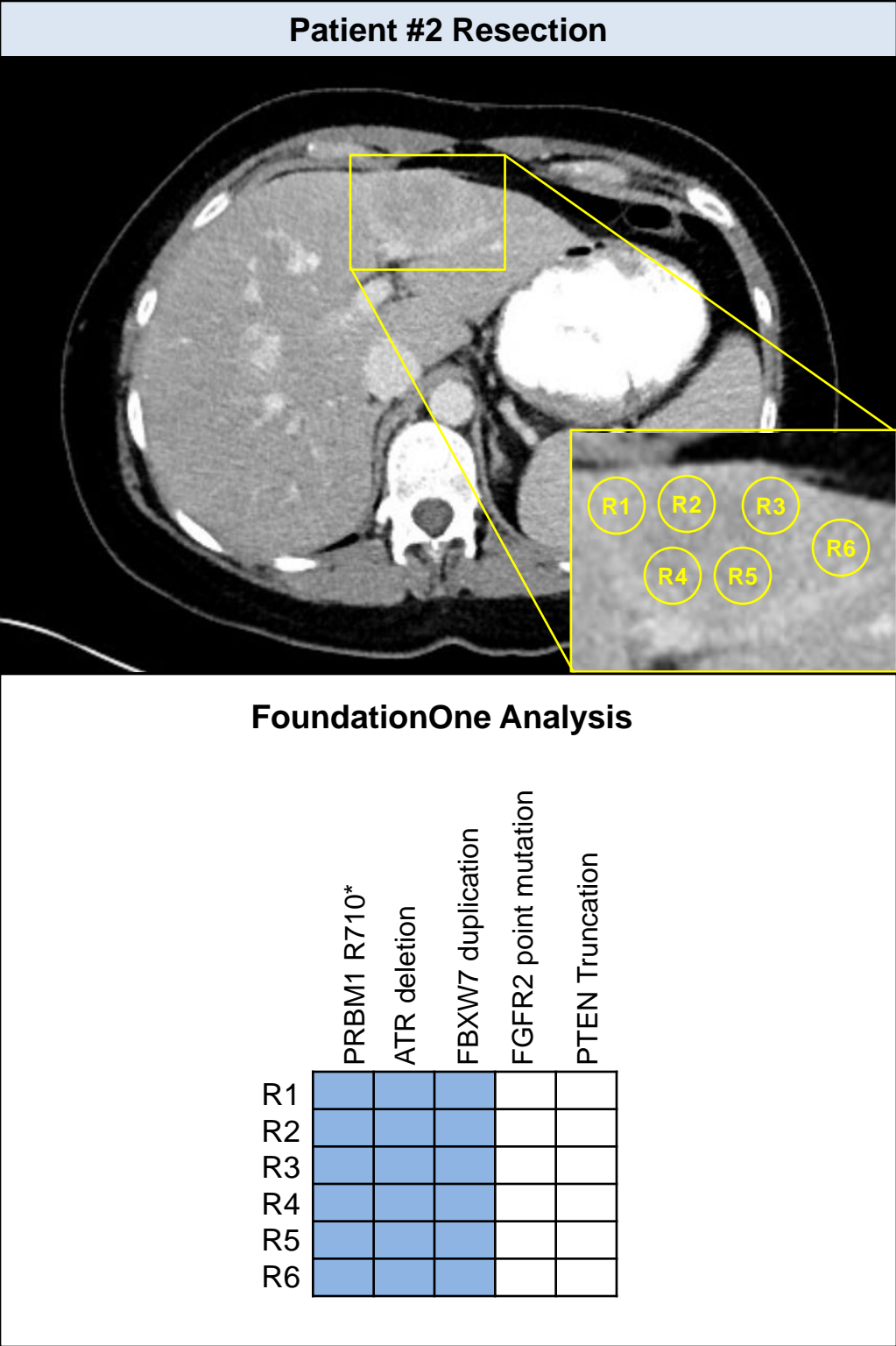
B



## Supplementary Figure S5. *PTEN* loss of heterozygosity (LOH) identified in Patient #2.

**A.** Intrachromosomal fusion event detected by FoundationOne assay in the post-progression biopsy sample from patient #2 and leading to *PTEN* LOH. **B.** Heatmap illustrating the relative copy number along chromosome 10 in normal tissue, pre-treatment and post-progression biopsies from Patient #1 and Patient #2 as determined by WES. Note: Patient #2 demonstrates loss of the entire long arm of chromosome 10q as an early event (pre-treatment).

# Supplementary Figure S6



**Supplementary Figure S6. Mutational analysis of original resection specimen from Patient #2.** *Top panel*, Axial contrast enhanced CT image of resected lesion from Patient #2. *Bottom panel*, Heatmap illustrating detected mutations in six spatially distinct pieces isolated from the resection specimen by FoundationOne assay.